

Adsorption of methylene blue from aqueous solutions using magnetic zero-valent iron-activated grape wastes: optimization and modeling

Davood Shahbazi^{a,c}, Seyyed Alireza Mousavi^{a,b,*}, Elham Noori^a

^aDepartment of Environmental Health Engineering, School of Public Health and Research Center for Environmental Determinants of Health (RCEHD), Kermanshah University of Medical Sciences, Kermanshah, Iran, emails: seyyedarm@yahoo.com/sar.mousavi@kums.ac.ir (S.A. Mousavi), dshahbazi1367@gmail.com (D. Shahbazi), elhamnoori67@gmail.com (E. Noori)

^bSocial Development and Health Promotion Research Center, Kermanshah University of Medical Sciences, Kermanshah, Iran
^cStudent's Research Committee, Kermanshah University of Medical Sciences, Kermanshah, Iran

Received 14 May 2019; Accepted 17 November 2019

ABSTRACT

In recent years, the adsorption process has been introduced as an effective method for dyes removal from aqueous solutions. In the present work, grape waste was used as a precursor for the preparation of a low-cost activated carbon through chemical activation. Then, to develop a solid-phase extraction process assisted by a magnetic field, magnetic adsorbent have produced by loaded zero-valent iron (Fe^0) on the powdered activated carbon. The physical and chemical properties of the AC/ Fe^0 adsorbent were characterized using Brunauer–Emmett–Teller, scanning electron microscopy and Fourier transforms infrared. The design of experiments was carried out based on the response surface methodology to evaluate the effects of variables including pH, contact time, initial concentration of methylene blue (MB) and adsorbent dosage. Analysis of variance results presented a high R^2 value of 80% for MB removal. The optimum condition was obtained at pH 11, adsorbent dosage 12.5 g/L, MB concentration 100 mg/L and contact time 90 min. To determine the adsorption kinetics, pseudo-first-order and pseudo-second-order models were investigated. The isotherm and kinetic studies showed that data were fitted to the Langmuir adsorption and pseudo-second-order models, respectively. The synthesized sorbent showed that the adsorption capacity of MB based on the Langmuir isotherm was found to be 44 mg/g.

Keywords: Activated carbon; Waste; Modeling; Dye; Magnetic nanoparticles

1. Introduction

With the trend of population growth and urbanization, the production of different types of wastewaters such as domestic and industrial wastewaters has increased. Among wastewaters, industrial wastewater due to a high concentration of pollutants such as nitrogen components [1,2], organic carbon [3], heavy metals [4,5], dyes and other contaminants attracted more attention of researchers to apply suitable methods for treatment [6]. Discharge of untreated wastewater containing dye from different

sources such as dyes stuff manufacturing, dyeing, printing, food plants, and textiles into the aqueous environment can cause problems such as damage the esthetic nature of the environment, creating anaerobic conditions, reducing the sunlight penetration, cancer and allergy [7]. Therefore, researchers have applied various technologies to remove dye from water and wastewater, such as Flocculation, anaerobic biological treatments, sonolysis, membrane separation, oxidative destruction via UV/ozone treatment, photocatalytic degradation. The aforementioned dye removal methods are effective but they are not cost-effective [8]. Adsorption as a

* Corresponding author.

simple and efficient technology with ease of operation and low initial cost has been widely used for dye removal from aqueous solutions [9]. However, activated carbon (AC) as an adsorbent has been applied for dye removal in bench-scale and full scale because of high adsorption capacity, but some shortcomings such as high cost and difficult way to separate from treated water-limited wide usage of AC. Researches during the last decades have attempted to find out cheap and efficient martial and also easy and rapid methods for the separation of adsorbents from solution. Recently, agricultural wastes have been studied for the development of cheap and more effective adsorbents [10–15]. Another disadvantage of using AC is that it has high usage costs. This has led researchers to search for natively available and cheap adsorbents, which make the process economically feasible [16]. The natural adsorbents have been used in the adsorption such as exhausted coffee ground [15], rice husk [11], oil palm fruits [12], pumpkin seed hull [10], apple wastes [13] and calcined eggshell [14]. On the other hand, the magnetic separation technique as an easy and fast method for separating magnetic adsorbents from aqueous solution has been performed in many research works [17–20]. In recent years, the combination of adsorption techniques and magnetism separation techniques has been widely used in the treatment of pollutants. Thus, combining the advantages of AC and magnetic particles as a promising way to overcome the shortcomings of conventional adsorbents and open new potentials for the achievement of effective magnetic adsorbent is an ongoing study [21].

This study has been carried out to remove methylene blue (MB) from aqueous solution using supported zero-valent iron on the activated carbon prepared by grape waste. The effects of main variables (pH, contact time, initial concentration of MB and adsorbent dosage) and their interaction on the process have been investigated. Furthermore, statistical analysis and modeling of data have been developed.

2. Materials and methods

2.1. Materials

All chemicals that have been used in this research were obtained from Merck Company, Germany without further purification. Methyl blue ($C_{16}H_{18}ClN_3S$; 319.85 MW) whit the chemical structure that is shown in Fig. 1 has been used as a cationic dye. H_3PO_4 (85 wt.%) has been used for chemical activation of carbon. Magnetic activated carbon carried out using Ferrous sulfate heptahydrate ($FeSO_4 \cdot 7H_2O$). The pH of solutions adjusted by sulfuric acid (0.1 N) and NaOH solutions (0.1 N).

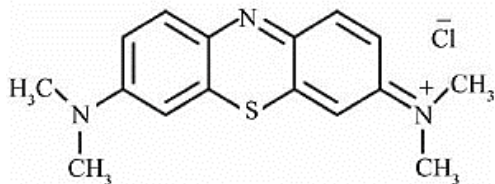


Fig. 1. Chemical structures of MB.

2.2. AC/Fe⁰ preparation

To prepare the adsorbent from grape waste, the leaves of the grapevine were harvested from Kermanshah vineyards, Iran. Then it was washed with water to remove any impurities such as toxins, dust. All prepared materials have been dried at 50°C for 3 h. After drying, the waste was cut into small pieces. At the first step of the activation phase, grape wastes were immersed in H_3PO_4 with a 1/10 mass ratio for 24 h. The chemical activated materials were placed at 700°C for 2 h. At the end of physicochemical activation, prepared AC was powdered using a mortar and passed through the sieve mesh size 50. The powder was mixed with distilled water and neutralized with sodium hydroxide and sulfuric acid 0.1 N. Finally, it was dried at 140°C for 4 h. The product was kept in a glass bottle to prevent moisture penetration. The co-precipitation method was used to synthesize of AC/Fe⁰. First, $FeSO_4 \cdot 7H_2O$ (100 mL) was added into AC (5 g), the solution was placed in a stirrer at 200 rpm for 30 min under nitrogen gas to remove oxygen in the environment. The obtained product was dried at 80°C. In the next step, $NaBH_4$ as a reducing agent was added to the solution to reduce the Fe(II) to zero iron. Finally, the AC/Fe⁰ immediately washed with distillation water and acetone after has been separated from aqueous solution by a magnet, and dried under nitrogen gas for 2 h.

2.3. Magnetic adsorbent characterization

The physicochemical properties of AC/Fe⁰ have been carried out by methods of Brunauer–Emmett–Teller (BET), scanning electron microscopy (SEM) and Fourier transform infrared (FTIR) using Quanta Chrome Corporation, USA, JEOL JSM 840A, Japan and ShimaDZU IR Prestige, Japan model, respectively.

2.4. Adsorption study

The adsorption study was conducted by mixing the desired amount of AC/Fe⁰ with 100 mL at different values of variables; initial MB concentration, initial pH, and contact time in Erlenmeyer flasks of 200 mL. After adjusting the pH of the solution using a pH-meter (WTW, Germany) all flasks have been shaken using a shaker (Orbital Company, Iran) at 200 rpm. At certain times, 3 mL of sample withdrawn and the MB residue was determined using a UV–Vis spectrophotometer (Jenway 6305, Germany) at 665 nm. The removal efficiency of MB (%) was calculated using the following equation:

$$\text{Dye removal (\%)} = \frac{(C_0 - C_t)}{C_0} \times 100 \quad (1)$$

where C_0 is the initial MB concentration and C_t is the final MB concentration.

2.5. Experiment design and data analysis

The experimental design and statistical analysis of data have been carried out by DOE software (version 8.00)

through response surface methodology (RSM) and analysis of variance (ANOVA). ANOVA is very crucial in validating the significance and adequacy of the model [22]. The standard RSM design called central composite design has the ability to minimize experiments and predict the effects of factors individually and in combination with each other. Furthermore, modeling and optimization of data can be developed based on variables [23]. Four factors were selected as independent variables viz. adsorbent dosage (0.25, 3.25, 6.25, 9.25, and 12.25 g/L), initial pH (3, 5, 7, 9, and 11) initial MB concentration (100, 200, 300, 400, and 500 mg/L), and contact time (10, 30, 50, 70, and 90 min). The values of independent variables have defined at 5 levels with three replications in 78 run (Table 1). The confidence level of more than 95% ($P < 0/05$) has been used to study the significance of analysis data and the developed model.

Table 1
Experimental conditions for MB removal

No.	A: time (h)	B: pH	C: adsorbent (g/L)	D: MB (mg/L)	Removal (%)
1	90	3	12.25	100	94
2	10	3	0.25	500	0.4
3	90	3	12.25	500	35.6
4	50	7	6.25	300	45.3
5	90	3	0.25	500	0.8
6	90	11	0.25	100	38
7	10	3	0.25	100	9
8	50	5	6.25	300	37
9	10	11	12.25	500	9.8
10	50	7	6.25	400	32.2
11	10	3	12.25	500	5.4
12	10	11	12.25	100	49
13	90	11	0.25	500	1.6
14	50	7	6.25	200	55.5
15	30	7	6.25	300	24.3
16	10	11	0.25	100	14
17	90	11	12.25	500	39
18	10	11	0.25	500	0.8
19	50	7	9.25	300	68
20	90	11	12.25	100	97
21	50	9	6.25	300	56.3
22	90	3	0.25	100	11
23	70	7	6.25	300	50.6
24	10	3	12.25	100	35
25	50	7	3.25	300	19
26	90	3	12.25	500	35
27	50	9	6.25	300	55.3
28	50	7	6.25	300	45.3
29	50	7	6.25	300	46.6
30	50	7	6.25	300	43.6
31	50	7	6.25	300	47
32	50	7	6.25	300	47.1
33	50	7	6.25	300	44.6

The three-dimensional and two-dimensional graphs have been applied to demonstrate the variable effects. A polynomial regression model based on independent factors according to Eqs. (2) can predict the efficiency of the process at different variable conditions [24].

$$Y = a_0 + \sum a_i x_i + \sum a_{ii} x_i^2 + \sum a_{ij} x_i x_j \quad (2)$$

where Y is the predicted response, a_0 , a_i and a_{ij} are respectively the regression coefficients for linear, quadratic effects and the coefficients of the interaction variables.

3. Results and discussion

3.1. AC/Fe⁰ characterization

The BET surface area of AC/Fe⁰ was 503.57 m²/g that indicates that most of the pores were blocked by the loaded Fe⁰ particles (Fig. 2). Fig. 3 demonstrates SEM images of AC/Fe⁰ composite. It is seen that the pores formed in various sizes and shapes. This structure has a large number of pores, and there is a good possibility for trapping of dye by adsorbed into the pores. It can be seen that the Fe⁰ particles with the particle size are nearly 700–2,000 nm in length dispersed over the AC matrix. The FTIR spectrum is a significant instrument to detect important functional groups present on the surface of materials that are capable of adsorbing organic pollutants. Fig. 4 demonstrates the FTIR spectra of AC/Fe⁰ composite. The characteristic adsorption bands of Fe–O were shown at 600 cm⁻¹ which confirmed the presence of Fe⁰ [25]. The bands at about 600–700 cm⁻¹ can be assigned to C–C stretching. The presence of a band at 1,414 cm⁻¹ belongs to C–H symmetric bending. The band at about 1,025 cm⁻¹ identifies the C=O groups [13]. The results of determining zero-point charge (pHzpc) show that it is 4.6 for AC/Fe⁰ that AC has been activated with phosphoric acid. This means that the surface charge of carbon for pH > 4.6 is negative and pH < 4.6 is positive. This value is in close agreement with the previous researches [26–28].

3.2. Process analysis and modeling

To study the relationship between response value and four parameters including initial pH, initial concentration

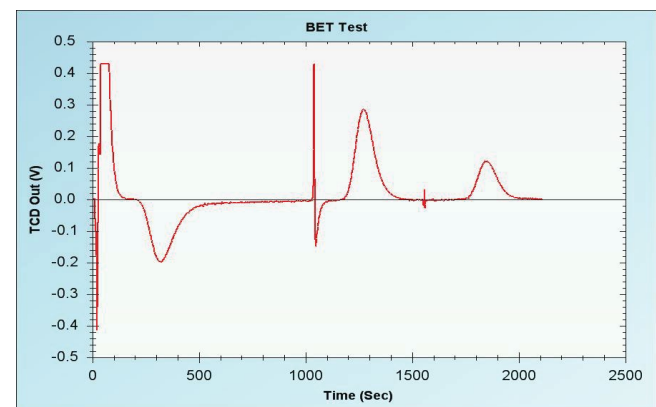


Fig. 2. BET plot of AC/ Fe⁰ composite.

of MB, contact time, adsorbent dosage a multiple regression analysis was used. Values of model terms $\text{Prob} > F < 0.0500$ indicate that factors are significant under selected conditions [29]. The model for yield revealed that *A, B, C, D, AC, AD, CD* are significant model terms. Initial concentration of MB and adsorbent dosage imposed the most significant effect on the MB removal, this was shown by their largest *F*-values as shown in Table 2. There is a good correlation between the experiment and predicted data with a correlation coefficient R^2 of 0.80 [30]. The best conditions for the responses yield were determined with the model predictor (Eq. (3)).

$$\text{Dye removal} = 33.90 + 12.32A + 4.23B + 19.03C - 14.68D + 8.73AC - 6.08AD - 5.50CD \quad (3)$$

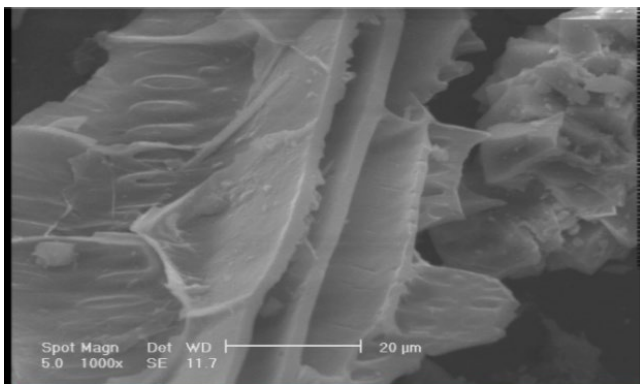


Fig. 3. SEM of AC/Fe⁰ composite.

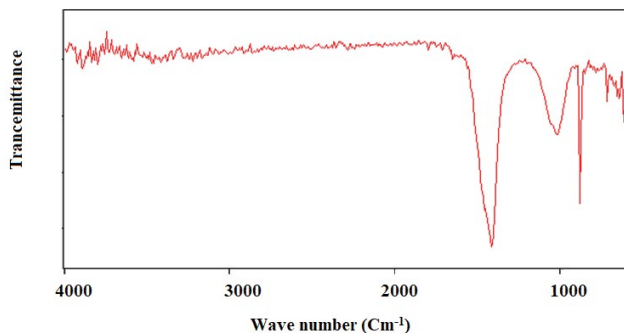


Fig. 4. FTIR spectra of AC/Fe⁰ composite.

Table 2
Results of statistical analysis

Source	Sum of squares	df	Mean square	F-value	p-value
Model	43,877.00	7	6,268.14	39.98	<0.0001
A-Time	7,511.01	1	7,511.01	47.91	<0.0001
B-pH	884.13	1	884.13	5.64	0.0203
C-Dosage	17,932.25	1	17,932.25	114.38	<0.0001
D-C	10,665.61	1	10,665.61	68.03	<0.0001
AC	3,655.78	1	3,655.78	23.32	<0.0001
AD	1,775.12	1	1,775.12	11.32	0.0012
CD	1,453.10	1	1,453.10	9.27	0.0033

The negative and positive signs in the equation depict antagonistic and synergetic effects of the respective variables respectively [31]. Residual vs. predicted response is shown in Fig. 5a. The plot should be a random scatter with a constant range of residuals across the graph. The adequacy of the model was confirmed by the normal probability plot of the residuals as represented in Fig. 5b. The perturbation plots for MB removal is shown in Fig. 5c. As can be seen, the pH curve shows a slow curvature indicating that this parameter has a slight effect on the MB removal. On the other hand, the remarkably steep curvatures in initial dye concentration and AC dosage curves indicate that the dye removal efficiency was sensitive to these variables.

3.3. Effect of initial MB concentration

The results of the present study confirm the effect of dye concentration on the adsorption process. Figs. 6a and b show the MB removal as a function of the initial concentration of MB and adsorbent dosage at the constant value of initial pH (7) and contact time (50 min). Generally, the percentage of dye removal increased with decreasing of initial dye concentration, it might be explained that at low concentrations of MB, the ratio of the available surface to initial number of dye molecules is higher and at higher concentrations of MB, the ratio of initial number of the existing surface to dye molecules become low [32]. Yagub et al. [33] studied the MB removal by using AC prepared by Pine leaves and described dye removal efficiency decreased by increasing the initial dye concentration. Namasivayam et al. [34] investigated Congo red removal using AC prepared by coir pith, the results show that the amount of dye adsorption increased with increasing the initial dye concentration [34].

3.4. Effect of adsorbent dosage

The 3D response surface plot contour plot of MB removal as a function of adsorbent dosage and initial concentration of MB at constant initial pH (7) and contact time (50 min) are shown in Figs. 6a and b. The results show that the dye removal efficiency from the solution increased by increasing adsorbent dosage from 0.25 to 12.25 g/L. The reason is that by increasing adsorbent dosage, because of the increase in active sites on the surface of AC/Fe⁰, more adsorbent surface was existing for adsorption, then making it easier for the

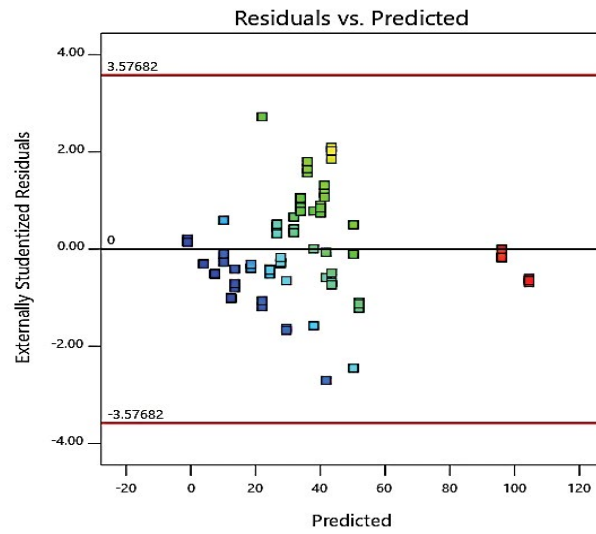
(a)

Design-Expert® Software

Removal

Color points by value of Removal:

0.4  97.5



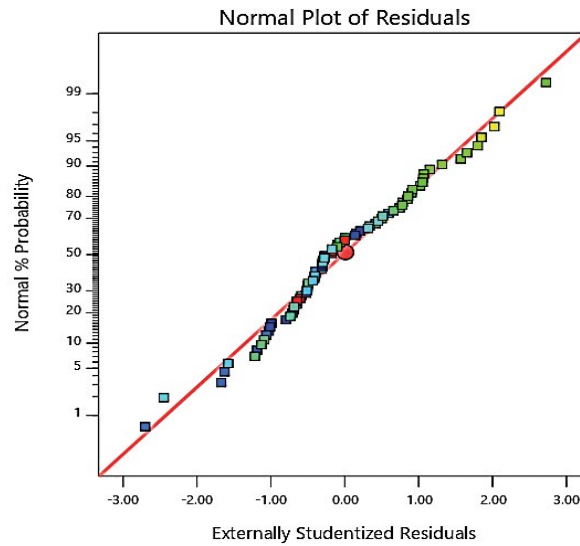
(b)

Design-Expert® Software

Removal

Color points by value of Removal:

0.4  97.5



(c)

Design-Expert® Software
Factor Coding: Actual

Removal (%)

Actual Factors

A: Time = 90.00
B: pH = 11.00
C: Dosage = 12.25
D: C = 500.00

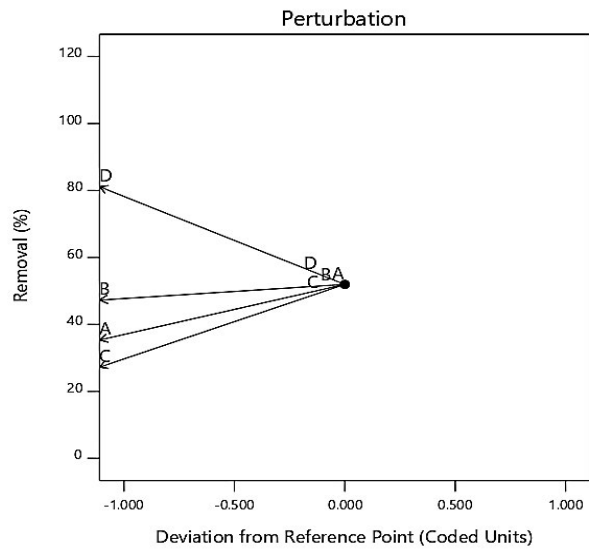


Fig. 5. (a) Residual vs. predicted response values plot, (b) normal probability plots, and (c) perturbation plots for MB removal.

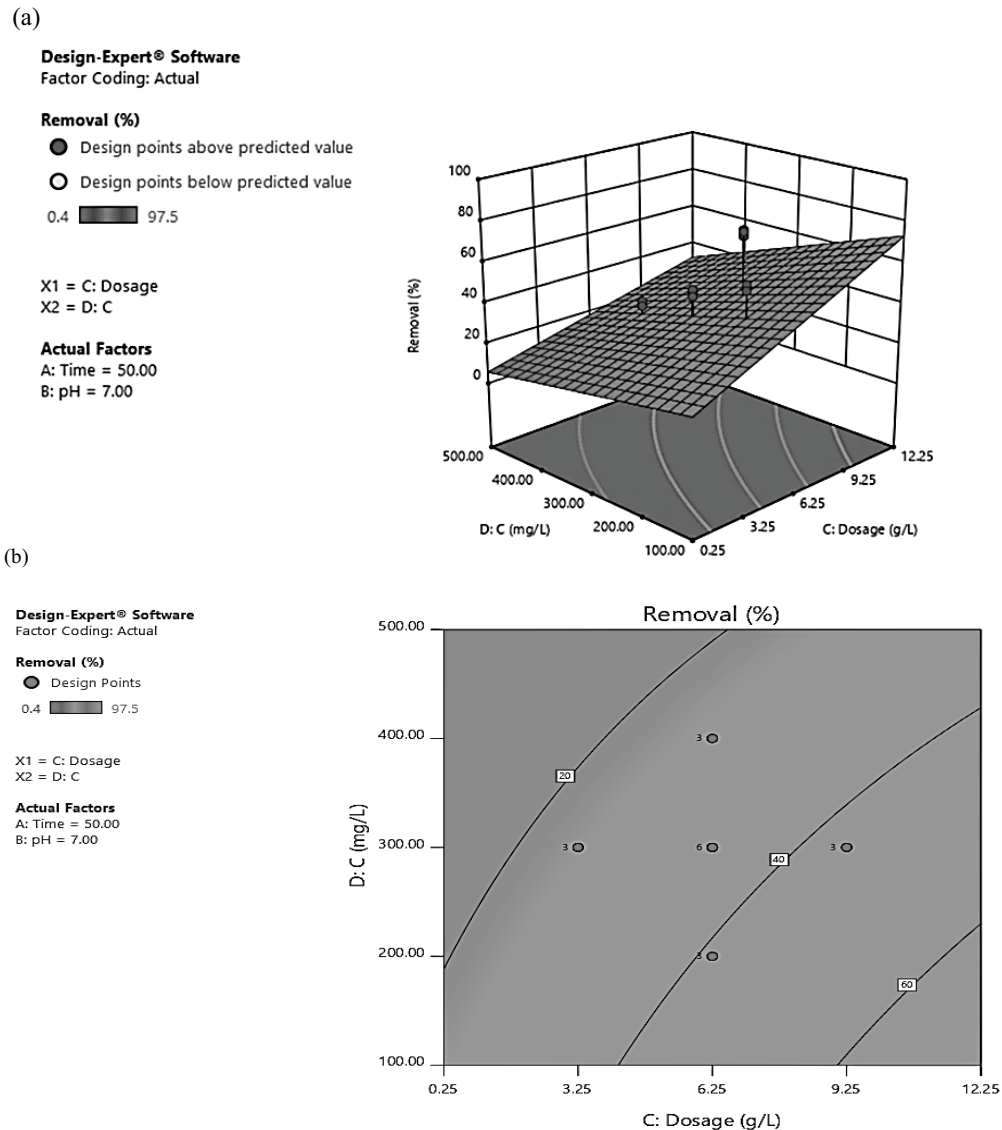


Fig. 6. (a) 3D response surface plot and (b) contour plots of MB removal efficiency as a function of adsorbent dosage and MB concentration at initial pH (7) and contact time (50 min).

adsorbate to penetrate the adsorption sites [32]. A similar result was previously shown for the MB removal by various adsorbents [34–37]. Senthilkumar et al. [36] found that dye adsorption increased by increasing adsorbent dosage from 0.02 g/50 ml to 0.20 g/50 ml. Also, Sen et al. [37] found that the amount of MB dye removal by pine cone was increased from 62.9% to 97.2% with the increase of adsorbent mass from 0.01 to 0.05 g.

3.5. Effect of initial pH

The pH value has a significant effect on the adsorption process due to the control of the protonation of the functional groups. The adsorption study was carried out by changing a pH range from 3 to 11. The 3D response surface plot and contour plot of the combined effect of initial pH and contact time on the removal of dye at constant

initial MB concentration (100 mg/L) and adsorbent dosage (6.25 mg/L) are shown in Figs. 7a and b. The results show that an increase in the initial pH of the solution causes to increase MB removal. This reason was maybe the static electricity mutual action between AC and dye which was controlled by pH value [38]. A similar observation was reported for MB removal from aqueous solutions in some of the previously published studies [39,40].

3.6. Effect of contact time

To determine the equilibrium time for maximum MB removal in the adsorption process, the contact time (10–90 min) between the dye and the adsorbent prepared, was investigated. The results are shown in Figs. 7a and b. According to Figs. 7a and b, the adsorption rate of MB increased with increasing the contact time from 10 to 90 min.

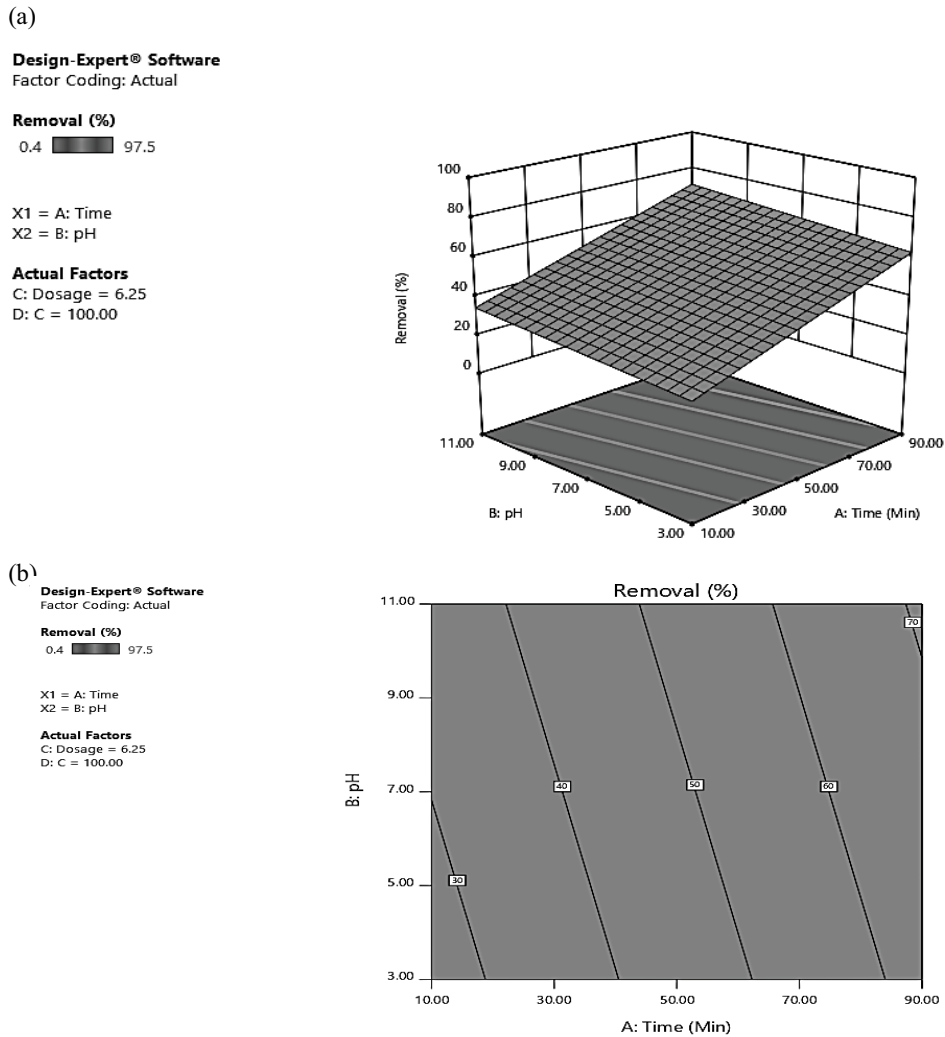


Fig. 7. (a) 3D response surface plot and (b) contour plots of MB removal efficiency as a function of contact pH and contact time at MB concentration (100 mg/L) and adsorbent dosage (6.25 g/L min).

The fast adsorption at the initial stage also may be because a large number of surface sites are available for adsorption but after a lapse of time, the remaining surface sites are difficult to be occupied [41,42]. The amount of dye removal increases with increasing contact time at all initial dye concentrations as reported by previous researchers [37,43,44].

3.7. Optimization

The graphical optimization represents the area of feasible response values in the factors space as shown in Fig. 8. The optimum region was identified based on MB removal. From Fig. 8, the optimum region is covered by contact time 90 min, initial MB 100 mg/L, AC dosage 12.25 mg/L and initial pH 11.

3.8. Kinetic studies

Predicting the rate of adsorption is one of the most important factors in the design of the adsorption system. To study the mechanisms of adsorption, different kinetic

models have been proposed [45]. In present work, the adsorption kinetics was studied with the pseudo-first-order and the pseudo-second-order models. The non-linear form of pseudo-first-order equation can be calculated using Eq. (4):

$$\log(q_e - q_t) = \log q_e - \frac{k_1}{2.303} t \tag{4}$$

where q_t and q_e are the amounts of dye adsorbed (mg/g) at time t (min) and equilibrium, respectively and k_1 is the rate constant of adsorption (min^{-1}).

The pseudo-second-order equilibrium adsorption model [31] is given as (Eq. (5)):

$$\frac{t}{q_t} = \frac{1}{k_2 q_e^2} + \frac{1}{q_e} t \tag{5}$$

where k_2 (g/mg min) is the rate constant of second-order adsorption. In recent years, a pseudo-second-order expression has been successfully used to the adsorption of dyes, metal ions, oils, herbicides, and organic substances from

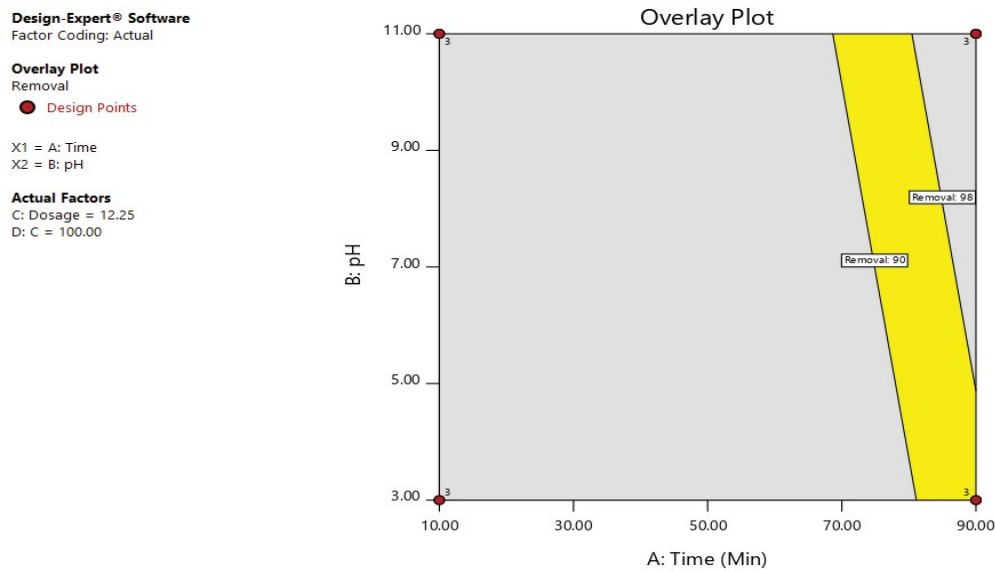


Fig. 8. Overlay plots for the optimal region; MB removal as a response.

aqueous solutions [46]. According to Fig. 9, the pseudo-second-order kinetic model ($R^2 = 0.993$) has a good fit with experimental data.

3.9. Equilibrium adsorption isotherm

The study of adsorption isotherms can provide information about the adsorbate distribution between the solid phase and the liquid phase when the adsorption process reaches equilibrium. Various mathematical models are used to describe the experimental data for adsorption isotherms. The equilibrium characteristics of this adsorption study were investigated with Freundlich and Langmuir equations. The Langmuir isotherm model assumes monolayer

coverage of adsorbent and adsorption occurs over specific homogenous sites on the adsorbent [47]. The linear form of the Langmuir isotherm model can be expressed as Eq. (6):

$$\frac{C_e}{q_e} = \frac{C_e}{q_m} + \frac{1}{q_m \times K_L} \tag{6}$$

where C_e (mg/L) is the equilibrium concentration of MB in solution, q_m and q_e are the monolayer adsorption capacity (mg/g), and amounts of MB (mg/g) adsorbed on adsorbent respectively. K_L is the Langmuir binding constant [48]. A plot of q_e against C_e gave a fitted curve, and the Langmuir constants were generated from the plot of sorption data. The linear form of the Freundlich isotherm is given as Eq. (7) [49]:

$$\ln q_e = \ln k_f + \frac{1}{n} \ln C_e \tag{7}$$

The n and K_f parameters in the Freundlich isotherm show adsorption intensity and the adsorption capacity of the system. Also, the value of $1/n$ shows the desirability of the sorbent/adsorbate systems.

The Langmuir and Freundlich isotherms obtained in the present work are shown in Fig. 10. The parameters obtained from Fig. 10 are summarized in Table 3. The results show that the constant equilibriums of dye removal are conformed to Langmuir isotherm with correlation coefficient $R^2 = 0.97$, so, monolayer type adsorption was obtained. The Langmuir isotherm model fits the data very good maybe because active sites are homogeneously distributed on the surface of the adsorbent. The coefficient of separation parameter R_L is one of the parameters of the Langmuir equation that describes the type of adsorption process. The type of isotherm was determined by the amount of R_L . In different amount of R_L including $R_L = 0$, $0 < R_L < 1$, $1 = R_L$, $1 < R_L$ the type of adsorption is irreversible adsorption, favorable

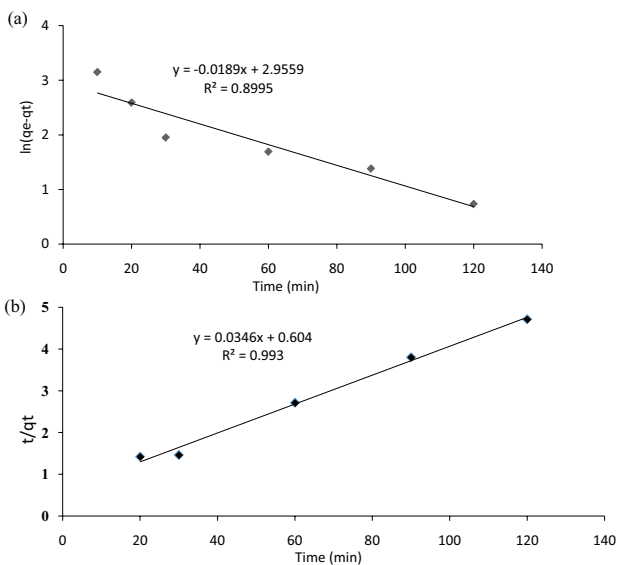


Fig. 9. (a) Pseudo-first-order and (b) pseudo-second-order kinetic plots for the adsorption of MB onto the prepared adsorbent.

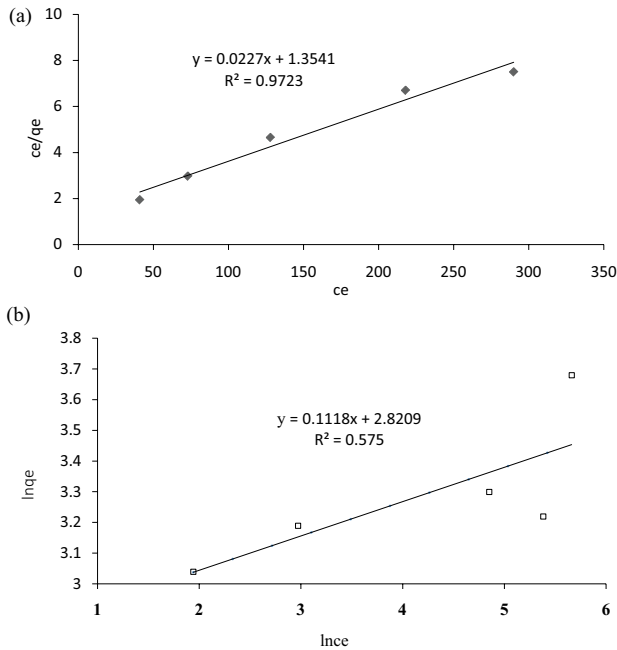


Fig. 10. Isotherm plots (a) Langmuir and (b) Freundlich and for MB adsorption onto the prepared adsorbent.

Table 3
Langmuir and Freundlich parameters for MB adsorption on the AC/Fe⁰

Langmuir			Freundlich		
R ²	q _m (mg/g)	B (L/mg)	R ²	K _f	1/n
0.9723	44.075	0.0167	0.57	16.64	8.94

adsorption, linear adsorption, and unfavorable adsorption, respectively [50]. According to the study of adsorption isotherms, the amount of R_L for MB adsorption is calculated to be 0.16, which indicates the MB is well absorbed on AC/Fe⁰ composite.

4. Conclusion

The AC/Fe⁰ adsorbent was prepared by loading nanoscale Fe⁰ onto AC and its performance for MB removal from aqueous solution was investigated by batch adsorption experiments. To obtain the optimal conditions for dye adsorption the effect of adsorption dosage, initial concentration MB, initial pH, and contact time on dye removal were investigated by RSM. The results showed that the adsorbent produced from grape waste has a good effect on the MB removal from aqueous solution. Also, the results show that the adsorption process follows the pseudo-second-order equation and adsorption data was well matched to the Langmuir models. This study provided a feasible approach for dye removal by magnetically separable adsorbent.

Acknowledgment

The authors thank the Kermanshah University of Medical Sciences for support of this research work.

References

- [1] S. Mousavi, S. Ibrahim, M.K. Aroua, Effects of operational parameters on the treatment of nitrate-rich wastewater by autohydrogenotrophic denitrifying bacteria, *Water Environ. J.*, 28 (2014) 556–565.
- [2] S.A. Mousavi, S. Ibrahim, Application of response surface methodology (RSM) for analyzing and modeling of nitrification process using sequencing batch reactors, *Desal. Wat. Treat.*, 57 (2016) 5730–5739.
- [3] P. Mohammadi, S. Ibrahim, M.S.M. Annuar, M. Khashij, S.A. Mousavi, A.A. Zinatizadeh, Optimization of fermentative hydrogen production from palm oil mill effluent in an up-flow anaerobic sludge blanket fixed film bioreactor, *Sustainable Environ. Res.*, 27 (2017) 238–244.
- [4] M. Khashij, S. Mousavi, M. Mehralian, M. Massoudinejad, Removal of Fe²⁺ from aqueous solution using manganese oxide coated zeolite and iron oxide coated zeolite, *Int. J. Eng. Trans. B*, 29 (2016) 1587.
- [5] A. Almasia, F. Navazeshkhaa, S.A. Mousavi, Biosorption of lead from aqueous solution onto *Nasturtium officinale*: performance and modeling, *Desal. Wat. Treat.*, 65 (2017) 443–450.
- [6] S. Mousavi, M. Mehralian, M. Khashij, S. Parvaneh, Methylene Blue removal from aqueous solutions by activated carbon prepared from *N. microphyllum* (AC-NM): RSM analysis, isotherms and kinetic studies, *NEST J.*, 19 (2017) 697–705.
- [7] S.A. Mousavi, S. Nazari, Applying response surface methodology to optimize the fenton oxidation process in the removal of Reactive Red 2, *Pol. J. Environ. Stud.*, 26 (2017) 765–772.
- [8] F. Keyhanian, S. Shariati, M. Faraji, M. Hesabi, Magnetite nanoparticles with surface modification for removal of methyl violet from aqueous solutions, *Arabian J. Chem.*, 9 (2016) S348–S354.
- [9] Y. Kim, J. Bae, H. Park, J.-K. Suh, Y.-W. You, H. Choi, Adsorption dynamics of methyl violet onto granulated mesoporous carbon: Facile synthesis and adsorption kinetics, *Water Res.*, 101 (2016) 187–194.
- [10] B. Hameed, M.I. El-Khaiary, Removal of basic dye from aqueous medium using a novel agricultural waste material: pumpkin seed hull, *J. Hazard. Mater.*, 155 (2008) 601–609.
- [11] V. Verma, A.K. Mishra, Kinetic and isotherm modeling of adsorption of dyes onto rice husk carbon, *Global NEST J.*, 12 (2010) 190–196.
- [12] O.S. Bello, Adsorptive removal of malachite green with activated carbon prepared from oil palm fruit fibre by KOH activation and CO₂ gasification, *S. Afr. J. Chem.*, 66 (2013) 32–41.
- [13] R.H. Hesas, A. Arami-Niya, W.M.A.W. Daud, J.N. Sahu, Preparation and characterization of activated carbon from apple waste by microwave-assisted phosphoric acid activation: application in methylene blue adsorption, *BioResources*, 8 (2013) 2950–2966.
- [14] R. Slimani, I. El Ouahabi, F. Abidi, M. El Haddad, A. Regti, M.R. Laamari, S. El Antri, S. Lazar, Calcined eggshells as a new biosorbent to remove basic dye from aqueous solutions: thermodynamics, kinetics, isotherms and error analysis, *J. Taiwan Inst. Chem. Eng.*, 45 (2014) 1578–1587.
- [15] K. Shen, M.A. Gondal, Removal of hazardous Rhodamine dye from water by adsorption onto exhausted coffee ground, *J. Saudi Chem. Soc.*, 21 (2017) S120–S127.
- [16] G. Vijayakumar, R. Tamilarasan, M. Dharmendirakumar, Adsorption, kinetic, equilibrium and thermodynamic studies on the removal of basic dye Rhodamine-B from aqueous solution by the use of natural adsorbent perlite, *J. Mater. Environ. Sci.*, 3 (2012) 157–170.
- [17] C.H. Xu, L.-j. Zhu, X.-H. Wang, S. Lin, Y.M. Chen, Fast and highly efficient removal of chromate from aqueous solution using nanoscale zero-valent iron/activated carbon (NZVI/AC), *Water Air Soil Pollut.*, 225 (2014) 1845.
- [18] A.M. Khalil, O. Eljamal, T.W. Amen, Y. Sugihara, N. Matsunaga, Optimized nano-scale zero-valent iron supported on treated activated carbon for enhanced nitrate and phosphate removal from water, *Chem. Eng. J.*, 309 (2017) 349–365.

- [19] H. Zhu, Y. Jia, X. Wu, H. Wang, Removal of arsenic from water by supported nano zero-valent iron on activated carbon, *J. Hazard. Mater.*, 172 (2009) 1591–1596.
- [20] X. Wu, Q. Yang, D. Xu, Y. Zhong, K. Luo, X. Li, H. Chen, G. Zeng, Simultaneous adsorption/reduction of bromate by nanoscale zerovalent iron supported on modified activated carbon, *Ind. Eng. Chem. Res.*, 52 (2013) 12574–12581.
- [21] L. Ai, Y. Zhou, J. Jiang, Removal of methylene blue from aqueous solution by montmorillonite/CoFe₂O₄ composite with magnetic separation performance, *Desalination*, 266 (2011) 72–77.
- [22] Z.N. Garba, W. Zhou, I. Lawan, M. Zhang, Z. Yuan, Enhanced removal of prometryn using copper modified microcrystalline cellulose (Cu-MCC): optimization, isotherm, kinetics and regeneration studies, *Cellulose*, 26 (2019) 6241–6258.
- [23] S.K. Behera, H. Meena, S. Chakraborty, B.J.I.J.o.M.S. Meikap, Technology, application of response surface methodology (RSM) for optimization of leaching parameters for ash reduction from low-grade coal, *Int. J. Min. Sci. Technol.*, 28 (2018) 621–629.
- [24] R. Saini, P. Kumar, Simultaneous removal of methyl parathion and chlorpyrifos pesticides from model wastewater using coagulation/flocculation: central composite design, *J. Environ. Chem. Eng.*, 4 (2016) 673–680.
- [25] L. Xiong, L. Zheng, J. Xu, W. Liu, X. Kang, Y. Wang, W. Wang, S. Yang, J. Xia, A non-enzyme hydrogen peroxide biosensor based on Fe₃O₄/RGO nanocomposite material, *ECS Electrochem. Lett.*, 3 (2014) B26–B29.
- [26] I. Shah, R. Adnan, W.S.W. Ngah, N. Mohamed, Iron impregnated activated carbon as an efficient adsorbent for the removal of methylene blue: regeneration and kinetics studies, *PLoS one*, 10 (2015) e0122603.
- [27] X. Lu, J. Jiang, K. Sun, X. Xie, Y. Hu, Surface modification, characterization and adsorptive properties of a coconut activated carbon, *Appl. Surf. Sci.*, 258 (2012) 8247–8252.
- [28] D. Borah, S. Satokawa, S. Kato, T. Kojima, Surface-modified carbon black for As(V) removal, *J. Colloid Interface Sci.*, 319 (2008) 53–62.
- [29] Z.N. Garba, A.A. Rahim, Optimization of activated carbon preparation conditions from *Prosopis africana* seed hulls for the removal of 2, 4, 6-Trichlorophenol from aqueous solution, *Desal. Wat. Treat.*, 56 (2015) 2879–2889.
- [30] E. Taghinezhad, V. Rasooli Sharabiani, M. Kaveh, Modelling and optimization of hybrid HIR drying variables for processing of parboiled paddy using response surface methodology, *Iran. J. Chem. Chem. Eng.* 38 (2018) 251–260.
- [31] A.H. Jawad, M.A.M. Ishak, A.M. Farhan, K. Ismail, Response surface methodology approach for optimization of color removal and COD reduction of methylene blue using microwave-induced NaOH activated carbon from biomass waste, *Desal. Wat. Treat.*, 62 (2017) 208–220.
- [32] H. Kaur, R. Kaur, Removal of Rhodamine-B dye from aqueous solution onto pigeon dropping: adsorption, kinetic, equilibrium and thermodynamic studies, *J. Mater. Environ. Sci.*, 5 (2013) 280–1838.
- [33] M.T. Yagub, T.K. Sen, H.J.W. Ang, Equilibrium, kinetics, and thermodynamics of methylene blue adsorption by pine tree leaves, *Water Air Soil Pollut.*, 223 (2012) 5267–5282.
- [34] C. Namasivayam, D. Kavitha, Removal of Congo Red from water by adsorption onto activated carbon prepared from coir pith, an agricultural solid waste, *Dyes Pigm.*, 54 (2002) 47–58.
- [35] M.A. Rahman, S.R. Amin, A.S. Alam, Removal of methylene blue from waste water using activated carbon prepared from rice husk, *Dhaka Univ. J. Pharm. Sci.*, 60 (2012) 185–189.
- [36] S. Senthilkumar, P.R. Varadarajan, K. Porkodi, C.V. Subbhuraam, Adsorption of methylene blue onto jute fiber carbon: kinetics and equilibrium studies, *J. Colloid Interface Sci.*, 284 (2005) 78–82.
- [37] T.K. Sen, S. Afroze, H.M. Ang, Equilibrium, kinetics and mechanism of removal of methylene blue from aqueous solution by adsorption onto pine cone biomass of *Pinus radiata*, *Water Air Soil Pollut.*, 218 (2011) 499–515.
- [38] Y. Bao, G. Zhang, Study of adsorption characteristics of methylene blue onto activated carbon made by *Salix psammophila*, *Energy Procedia*, 16 (2012) 1141–1146.
- [39] R. Han, W. Zou, W. Yu, S. Cheng, Y. Wang, J. Shi, Biosorption of methylene blue from aqueous solution by fallen phoenix tree's leaves, *J. Hazard. Mater.*, 141 (2007) 156–162.
- [40] M.A. Bedmohata, A.R. Chaudhari, S.P. Singh, M.D. Choudhary, Adsorption capacity of activated carbon prepared by chemical activation of lignin for the removal of Methylene Blue dye, *Int. J. Adv. Res. Chem. Sci.*, 2 (2015) 1–13.
- [41] M.N. Idris, Z. Ahmad, M.A. Ahmad, Adsorption equilibrium of malachite green dye onto rubber seed coat based activated carbon, *Int. J. Basic Appl. Sci.*, 11 (2011) 38–43.
- [42] M. Foroughi-Dahr, H. Abolghasemi, M. Esmaili, A. Shojamoradi, H. Fatoorehchi, Adsorption characteristics of Congo red from aqueous solution onto tea waste, *Chem. Eng. Commun.*, 202 (2015) 181–193.
- [43] M.K. Purkait, A. Maiti, S. Das Gupta, S. De, Removal of congo red using activated carbon and its regeneration, *J. Hazard. Mater.*, 145 (2007) 287–295.
- [44] K.Y. Foo, B.H. Hameed, Microwave assisted preparation of activated carbon from pomelo skin for the removal of anionic and cationic dyes, *Chem. Eng. J.*, 173 (2011) 385–390.
- [45] Y.S. Ho, Review of second-order models for adsorption systems, *J. Hazard. Mater.*, 136 (2006) 681–689.
- [46] J. Goel, K. Kadirvelu, C. Rajagopal, V.K. Garg, Investigation of adsorption of lead, mercury and nickel from aqueous solutions onto carbon aerogel, *J. Chem. Technol. Biotechnol.*, 80 (2005) 469–476.
- [47] I. Langmuir, The adsorption of gases on plane surfaces of glass, mica and platinum, *J. Am. Chem. Soc.*, 40 (1918) 1361–1403.
- [48] Z. Cheng, L. Zhang, X. Guo, X. Jiang, R. Liu, Removal of Lissamine rhodamine B and acid orange 10 from aqueous solution using activated carbon/surfactant: process optimization, kinetics and equilibrium, *J. Taiwan Inst. Chem. Eng.*, 47 (2015) 149–159.
- [49] S. Yakout, A. Daifullah, S.J.A.S. El-Reefy, Technology, adsorption of naphthalene, phenanthrene and pyrene from aqueous solution using low-cost activated carbon derived from agricultural wastes, *Adsorpt. Sci. Technol.*, 31 (2013) 293–302.
- [50] A. Almasi, S.A. Mousavi, A. Hesari, H. Janjani, B. Sciences, Walnut shell as a natural adsorbent for the removal of Reactive Red 2 form aqueous solution, *J. Basic Appl. Sci.*, 10 (2016) 551–555.